J Sustain Const Mater Technol, Vol. 8, Issue. 2, pp. 120–133, June 2023

Journal of Sustainable Construction Materials and Technologies
Web page info: https://jscmt.yildiz.edu.tr
DOI: 10.47481/jscmt.1256454

JSCMT
Journal of Sustainable Construction Materials and Technologies

Research Article

Strengthening of RC frames with infill walls using high strength lightweight concrete panels

Hakan KOMAN*

Department of Civil Engineering, İstanbul Aydın University, İstanbul, Türkiye

ARTICLE INFO

Article history
Received: 25 February 2023
Revised: 30 May 2023
Accepted: 31 May 2023

Key words:
Abaqus, concrete panel, epoxy, numerical analysis, polyurethane binder, RC frame, strengthening

ABSTRACT

This study proposed a practical seismic retrofit method for RC frames. For this purpose, a quasi-static loading was applied to 8 RC frames in finite element analysis software, Abaqus, and frames were pushed 45 mm laterally. High-strength fiber-reinforced lightweight concrete panels strengthened infill walls inside the RC frames. To apply them to the walls, epoxy binder and polyurethane binder were used, and their behavior was compared. Using panels increased the lateral load capacity of the whole frame according to the numerical analysis performed with Abaqus. In the worst case, the retrofitted frame carried approximately two times the traditionally infilled frame's capacity. In the best case, the RC frame carried 4.29 times the lateral load traditionally infilled frame. Polyurethane binder prevented the separation of panels from walls and provided a ductile behavior to frames even in large drifts.

Cite this article as: Koman, H. (2023). Strengthening of RC frames with infill walls using high strength lightweight concrete panels. *J Sustain Const Mater Technol*, 8(2), 120–133.

1. INTRODUCTION

Strong earthquakes cause significant damage to buildings, and human lives are lost. In the past, Northridge 1994, Kocaeli 1999, and Kobe 1995 earthquakes caused significant damages. Recently in Pazarcık, Kahramanmaraş, an earthquake magnitude of 7.7 caused extensive damage. Only 9 hours later, another earthquake happened in Elbistan, Kahramanmaraş, with a magnitude of 7.6. The distance between the two earthquakes' locations is only around 100km. This means the modern seismic code approach, which relies on the ductility of RC structures to save lives in earthquakes, could not guarantee the survival of buildings even if they were built according to the code provisions. Also, it was observed that RC buildings were not ductile enough to consume the earthquake energy. The lack of quality of RC buildings and the lack of quality in controlling RC buildings in Turkey were observed in past earthquakes also. A big earthquake is expected to happen in İstanbul soon.

One way to prepare for such a big earthquake is to use seismic retrofit methods to strengthen the risky building stock. However, the difficulties of applying seismic retrofit methods affect the decisions of residents or building owners. Usually, they do not want to leave the building for a long time during the retrofitting process. Seismic retrofit of an RC building is not affordable for many residents. A quick and practical seismic retrofit method is needed. A method that can be easily applied, like a simple repair inside the flat, is needed. Previously, retrofitting the infill walls inside RC frames by using CFRP strips was proposed, and a behavior model was developed for the retrofitted frames. The model was verified experimentally by using the results of two sovereign studies. Then by using this model, the analysis of a three-story RC structure (which was built in the 1970s) was performed, and it was concluded that, according to the push-over results, CFRP-based retrofitting of infill walls increased the stiffness and strength capabilities of the structure without needing any other retrofitting strategy [1]. CFRP material

***Corresponding author.**
*E-mail address: hakankoman@hotmail.com

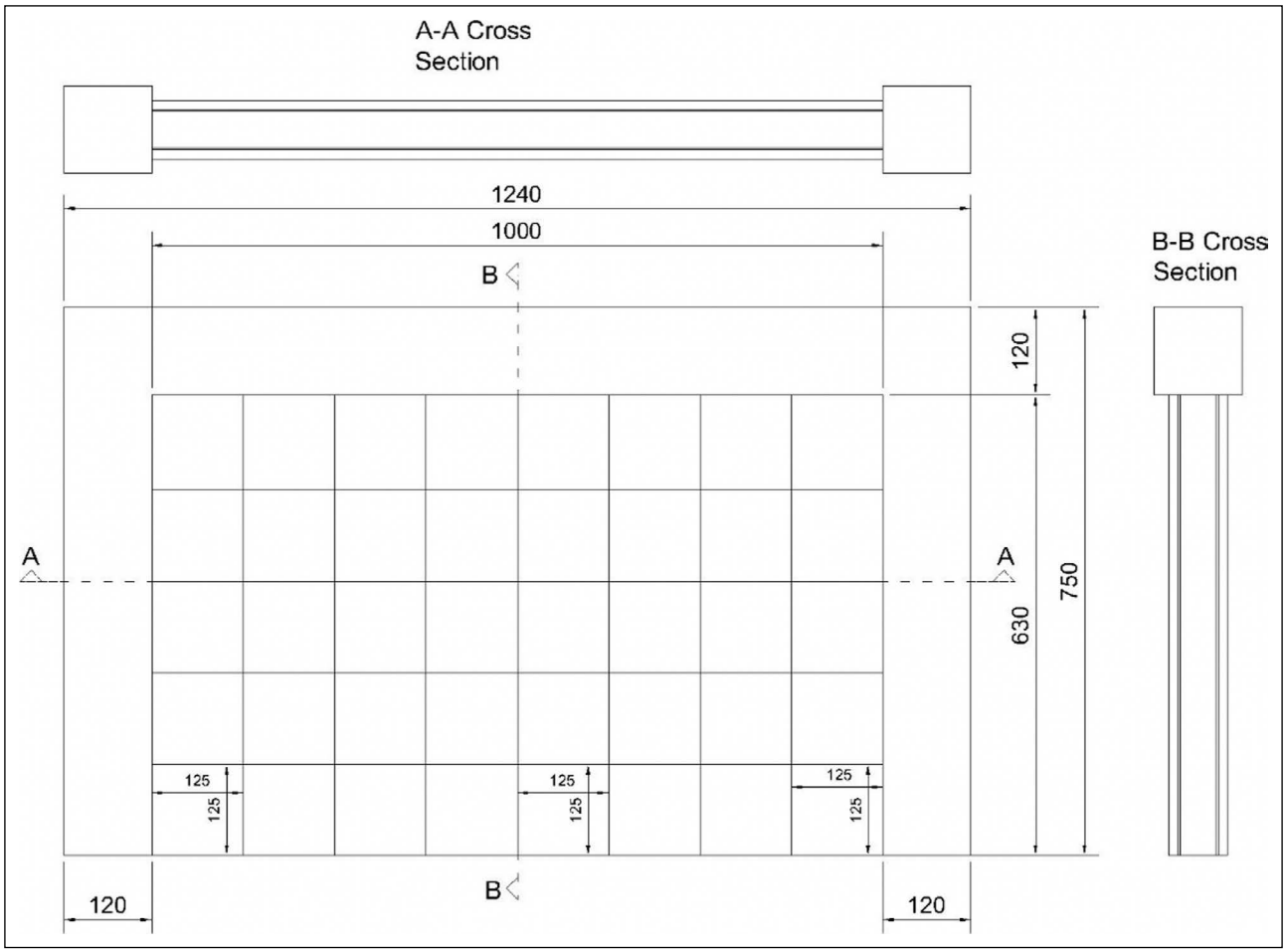

Figure 1. Proposed retrofitting of infill wall inside RC frame.

is beneficial for strengthening purposes. However, its cost limits the usage of the material widely. In another past study, a method was proposed, and experiments were performed to test the idea. The idea was to use precast RC panels to strengthen the infill walls inside the RC frames [2]. Although this was a practical idea, it can still be improved. Instead of precast RC panels, which need quality workmanship to be produced, another panel type can be used. Also, different types of binders rather than epoxy must be considered. So, in this study, an attempt was made to improve the idea, and fiber-reinforced high-strength lightweight concrete is used for panels, and the effect of polyurethane binder between wall and panel was investigated. The suggested infill wall strengthening and Abaqus modeling of the strengthened wall is seen in Figure 1 and Figure 2. In the strengthening process, panels with two different thicknesses (5 cm, 3 cm) and 0.5 m x 0.5 m dimensions were assumed for the study. The thickness of the binder between the wall and panels is assumed as 1cm. A scaled frame was used in the analysis, which is why all dimensions were divided by 4. Epoxy is compared with the highly deformable polyurethane binder. Highly deformable polyurethane binders were proposed by a past study to reduce the stress concentrations in structural elements in seismic retrofitting of masonry structures, and it was seen that such kind of binders provides some amount of ductility to structures also [3]. Abaqus analysis was made only in this

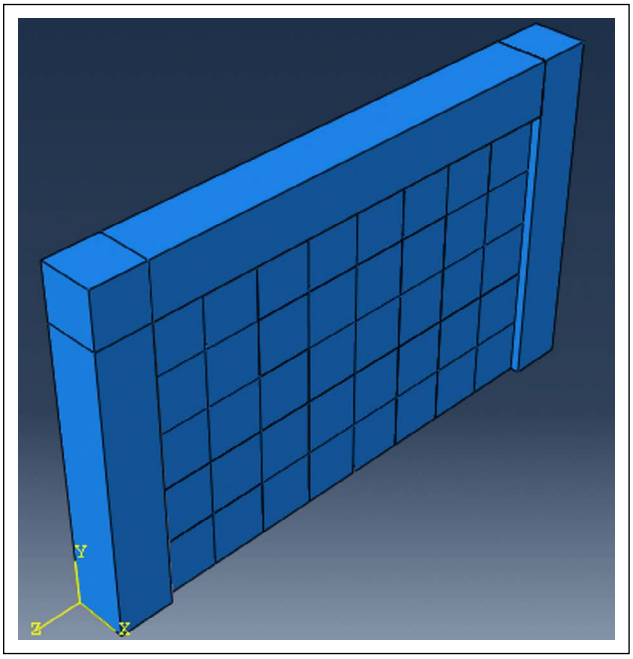

Figure 2. Demonstration of Abaqus modeling of RC frame with infill wall and attached panels.

study, and no experiments were performed for frames. However, the material properties were taken from the experimen-

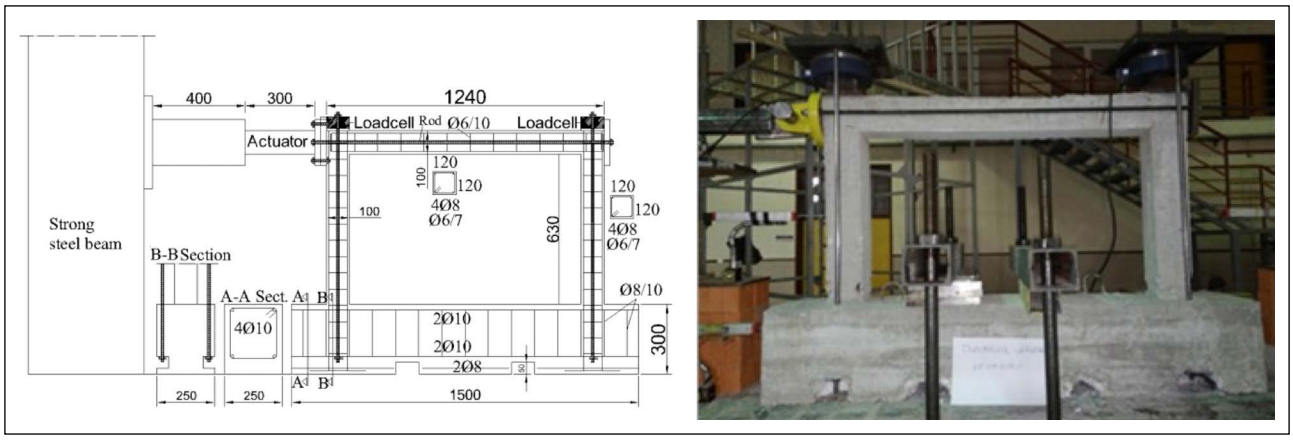

Figure 3. The scaled frame used in the past study [4].

tal work of past studies. In past studies, Abaqus is a powerful tool to perform a finite element method (FEM) analysis to obtain results very close to the experimental work [4].

2. NUMERICAL ANALYSIS

The 1/4 scaled RC frame used in a past study [4] was used again to test the effect of panels and polyurethane binder. The frame in the previous study was designed by assuming a 600kN load for each column and a 250kN lateral load. In the design of the frame, columns and beams with dimensions of 40 x 40 cm were assumed, and rebar design was performed following the 2018 Turkish earthquake code (TSC 2018). The height of the assumed frame is 3m, and the bay length of the frame is 4m. Due to the constructive reasons for the experimental part of the past study [4], the beam and columns are assumed to be in the same dimension, which leads to the lack of a robust column-weak beam mechanism. This fact is also considered in this study because it is well-known that buildings without strong column-weak beam collapse mechanisms exist in the risky building stock. After structural analysis, the following internal forces were obtained for the RC design, N_d=700KN (axial), V_d=126kN (shear), M_d=206kNm (moment) for the column, and V_d=92kN, M_d=172kNm for the beam. A 1/4 ratio scaled the frame by using a practical proper modeling approach but instead of 10 x10cm dimensions, a frame of 12 x 12cm with a height of 0.75m and width of 1m is obtained due to constructive reasons for the experimental work in the past study [4]. The RC design was re-checked for the new size, and no change was found. The stir-up length was taken as 3.5 and 3cm in columns and beam ends, respectively. According to the practical proper modeling approach, the distances between rebars were also assumed to be scaled by the scaling ratio. The details of the practical, accurate modeling approach were explained in a past study [5]. It is known that, in practice, there have been problems with concrete pouring and curing of concrete in Turkey. This study changed the properties of the frame's concrete to represent the risky building stock. Concrete's cubic compressive strength is assumed as 17.5Mpa (Abaqus use cubic specimen result). The details of the RC frame can be seen in Figure 3 [4].

Bare frames without infill walls, frames with traditional infill walls, and frames with infill walls and panels were analyzed in Abaqus. In frames with infill walls and panels, the effect of binder material is analyzed using epoxy and polyurethane-based adhesive. Eight types of frames were analyzed under vertical and horizontal loading. The first type of frame was the bare frame without any infill walls. The second type of frame included traditional infill walls only. In the third type of frame, panels were attached to the infill wall with an epoxy layer as a binder material. Also, panels surrounded by RC frames were assumed to be anchored to the frame members. In the fourth type of frame, differently than the third type, no anchorage was assumed between panels and frame members. The fifth type of frame was prepared like the third frame; however, the binder material was changed, and polyurethane (polymer) material was used. In the sixth type of frame, panels were attached to the infill wall using a polymer layer between the wall and panels, and no panel was assumed to be anchored to the frame members. In the seventh type of frame, panel thickness was decreased, and a 3 cm panel was assumed for an actual structure. Because of the scaled model in this study, a 7.5mm panel was used in the analysis, and panels surrounded by frame members were assumed to be anchored to frame members. Again, panels with 7.5mm thickness were used in the eighth frame, but differently than the seventh frame, polyurethane (polymer) binder was assumed as a binder material. In all the frames, 5 MPa axial loading was applied on columns, and 0.21 MPa loading was applied on the beam's upper surface to represent an actual loading on a fundamental structure. The base of the frame was assumed as fixed support, and the frame was pushed 45mm laterally.

In Abaqus, the analysis could be done by implicit analysis. However, explicit dynamic analysis is used. Detailed dynamic analysis in Abaqus uses the central difference method to solve the equation of motion. This method has a relatively low computational cost because the stiffness, mass, and damping matrices are not formed for every iteration, and the displacements in I+1 step are found by using the displacements in I and I-1 steps. Significant computational power is not needed. Detailed dynamic analysis can be used under some circumstances for quasi-static loading

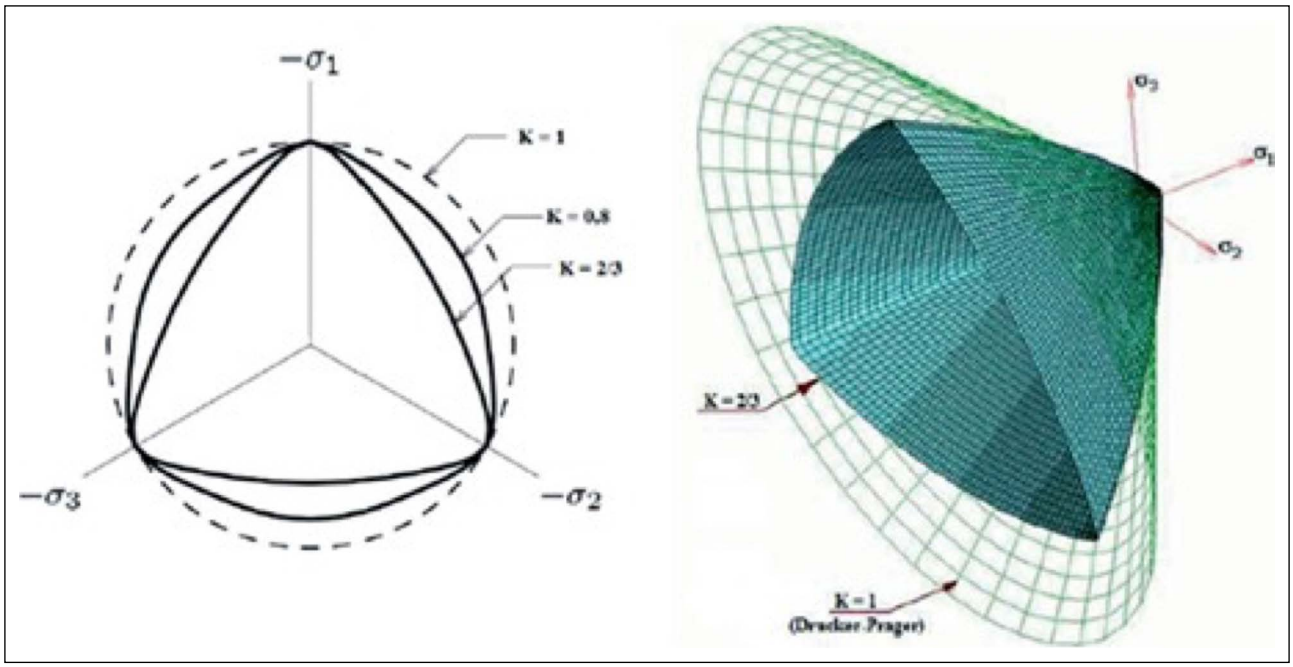

Figure 4. CDP model [6].

because a static problem is changed to an emotional one. However, if the inertial forces were kept under a specific level, the problem can be considered static. After the analysis, this can be determined by checking the kinetic energy/ total internal energy ratio. The analysis is considered static loading if this value is under or equal to 0.10. The details were explained in a previous study [5].

2.1. Material Properties and Modelling

2.1.1. Modelling of Concrete

In Abaqus software, the CDP model is available to model concrete. In literature, there are several failure theories to predict if a material will undergo plastic deformations under stress. This can be done by separating the stress tensor into hydrostatic and deviatoric components. Von Misses' theory assumes that the hydrostatic part of stresses does not cause plastic deformations. However, in the Drucker-Prager model, hydrostatic part is also taken into account. The CDP model is derived from Drucker -Prager model. As seen in Figure 4, K coefficient determines the modification. In CDP model K is equal to 2/3, whereas in Drucker Prager model it's equal to 1.

The stress-strain relationship of concrete is considered as shown in Figure 5 in Abaqus [7]. In Figure 5, dc parameter indicates the effects that changes the slope of stress strain diagram of concrete in compression. The stress and inelastic strain values are used in Abaqus in CDP model. Two kinds of concrete were modelled in this study. One of them is RC frame's concrete and the other one is a kind of high strength lightweight concrete used for the panels.

The properties of the concrete for frame were taken from a previous study where a real RC bridge's concrete was modelled [8]. The compressive strength of concrete was 17.5Mpa (cubic specimen strength is used in Abaqus). Young modulus of concrete for frame was taken as

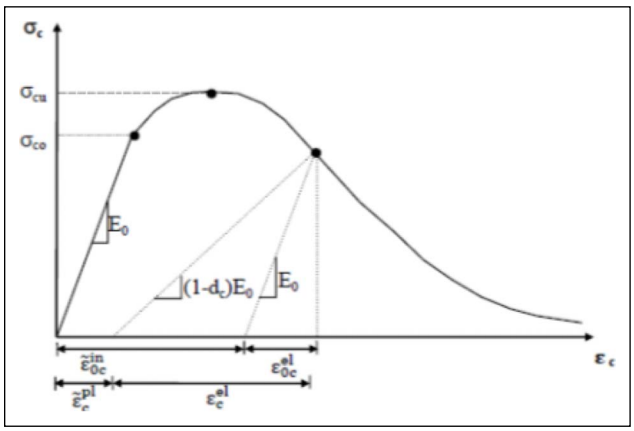

Figure 5. Stress strain relationship of concrete [7].

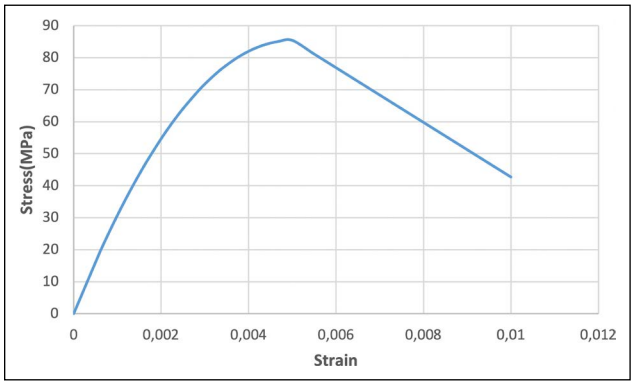

Figure 6. Stress strain relationship of high strength lightweight concrete.

19662MPa. The dilation angle, was taken as 40 degrees for concrete. Eccentricity determines the ratio of concrete's tensile strength to concrete's pressure strength and it was taken as 0.1. fbo/fco ratio was assumed as 1.14. fbo expresses the

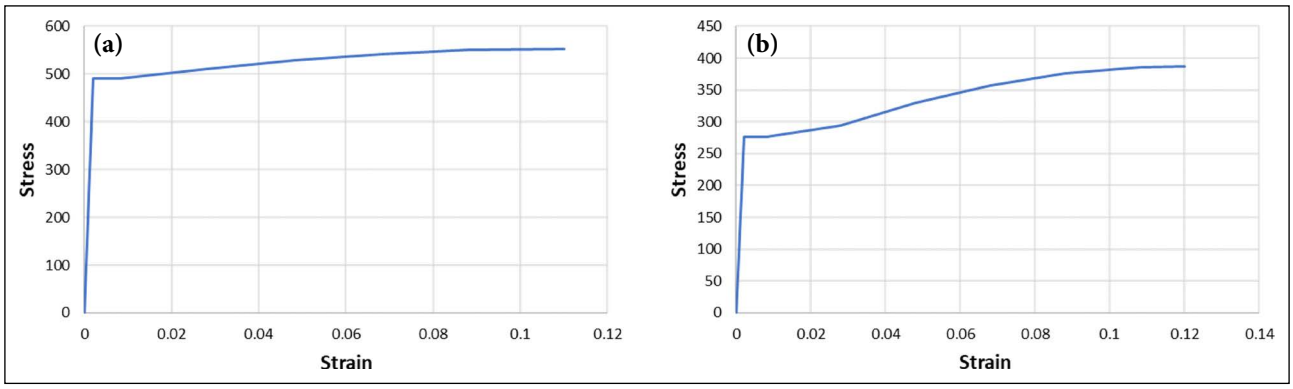

Figure 7. **(a)** Stress strain relationship of S420b; **(b)** Stress strain relationship of SAE for confinement [4].

strength of concrete in the situation when stresses acting two dimensionally. fco is the strength of concrete when it's loaded one dimensionally.

For panels, a steel fiber reinforced, high strength, lightweight concrete which is produced with expanded clay aggregates was used. The properties of the concrete were taken from a past study. In the past study, the different mixtures were used to produce lightweight concrete and the effect of steel fiber amount inside the concrete was investigated. It was seen that the compressive strength of concrete is affected by the aspect ratio of fibers and fiber volume fraction. Test results showed that a high strength lightweight concrete with a compressive strength of 85.4MPa and with a density of 1966kg/m^3 can be produced by using 520kg/m^3 cement amount and 2% fiber volume fraction. The modulus of elasticity of this concrete was calculated as 28000 MPa in the study, and an equation was developed for finding it. Poisson ratio of this concrete was taken as 0.16 [9]. Dilation angle was assumed as 38 degrees, eccentricity as 0.1, f_{bo}/f_{co} as 1.16. Based on the strength values obtained experimentally in the past study, the stress strain relationship of the concrete were determined by using Hognestad model which is widely known. The strain corresponding to maximum stress was assumed as 0,0022 in Hognestad model. In Abaqus, inelastic strains were implemented to CDP model. The stress strain relationship of high strength lightweight concrete (based on the results of a previous experimental study) with steel fibers with an amount of 156kg/m^3, can be seen in Figure 6.

2.1.2. Modelling of Steel

The properties of steel rebars were taken from a previous study. The producers' tensile test results (which were performed according to TS708) were utilized to predict the behaviour of steel. The yield strength and tensile strength of S420b, utilized as 8mm bars in RC frames, were determined to be 491MPa and 553MPa, respectively based on the experimental results of producer company. The yield strength and tensile strength of SAE 5.5 steel, which was employed as confinements in RC frames, were calculated as 277 MPa and 387 MPa, respectively. Effects of strain hardening were taken into consideration during modelling. The stress strain equations as described in section 5 of Turkish Seismic Code 2018 was taken into account as seen in Figure 7, 8. In the model described in Figure 8, f_{sy} is the yield strength, f_{su} is the ultimate strength, ε_{sy} is the yield strain, ε_{su} is the ultimate strain of the steel material and ε_{sh} describes the strain at the beginning of strain hardening. Ultimate strains for steel materials were taken as 0.11 for S420b and 0.12 for SAE steel in modelling based on the experimental results mentioned in past study [4].

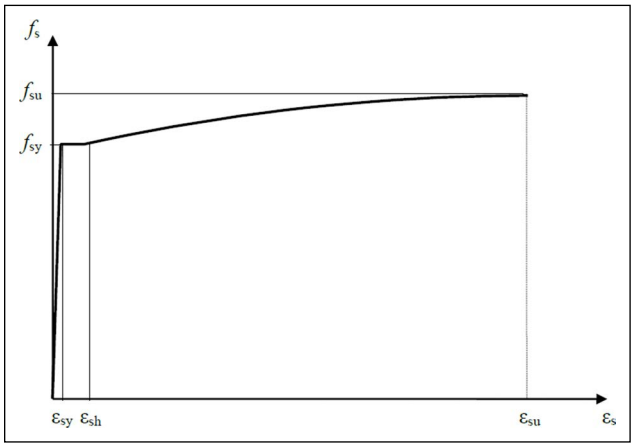

Figure 8. Stress strain relationship for nonlinear analysis of steel as described in Turkish Seismic Code 2018.

2.1.3. Modelling of Infill Wall

The infill walls inside a frame can be modelled by using micro modelling approach or macro modelling approach. For micro modelling approach, the mechanical properties of brick, mortar and brick-mortar interface must be determined separately. Macro modelling can be done by homogenization of wall by analysing a small portion of wall or using some formulas given in codes. In a previous study, traditional hollow brick's mechanical properties were determined experimentally. The average compressive strength, modulus of elasticity and tensile strength of hollow bricks was determined as 3.56MPa, 1111.49MPa, 0.9MPa respectively [4].

The mortar used to build the wall was a 1:2:9 (cement: lime: sand) mortar. In Abaqus, the CDP model was utilized to simulate the behaviour of mortar. Unlike concrete modelling, the dilation angle was determined to be 36.4 degrees. Mortar's compressive strength, young modulus, Poisson's ratio, and tensile strength were found to be, respectively, 4.97MPa, 700MPa, 0.157, and 0.257MPa experimentally [4].

Based on the results of experiments, quasi-static loading of an RC frame was performed in Abaqus by using micro modelling approach of walls and it's compared with macro modelling approach. There was an acceptable small discrepancy between the results of two analysis. However, after large lateral displacement of RC frame discrepancy increased. Compressive (Equation 1) and tensile strength (Equation 2) of infill wall in macro modelling approach was found in this study by using the following formulas based on Eurocodes [4]:

$$f_{ck}=0.4 \times 3.56^{0.75} \times 5^{0.25}= 1.57MPa \quad (1)$$

$$f_{ctk}=0.4 \times 0.9^{0.75} \times 0.257^{0.25}= 0.26MPa \quad (2)$$

And the modulus of elasticity of the infill wall was determined by the homogenization of a small portion of the wall. It's assumed as 1012.24MPa. The details of the experimental work and determination of young modulus can be seen in the previous study [4].

2.1.4. Modelling Of The Binders Between Panels and Wall

Two kinds of binders were used between panels and the wall in this study. One of them is epoxy and the other one is a two-component polyurethane binder called polymer pm. It's a two-component binder which can be applied as a fluid first but it gets hardened quickly in a few minutes after mixing with other component. When hardened it becomes a rubber like material. In a previous study, epoxy and a polyurethane binder were compared for seismic retrofit of masonry structures by using fiber reinforced polymers (FRP) [10]. In this study, Mooney Rivlin theory was proposed to model the behaviour of polyurethane binder. Mooney Rivlin theory is a theory used to model the hyper elastic materials like rubber. The stress strain curve of hyper elastic materials is not linear. Also, after large strains there is an increase in the stress. So classical theories are not used to explain the behaviour of hyper elastic materials. Instead, strain energy function which indicates the area under the stress strain curve is defined. The Mooney Rivlin theory is shown in the following equations (3–7), as indicated in a previous study [10]:

$$W^{M-R} = C_{10}\left(\Delta^2 + \frac{2}{\Delta} - 3\right) + C_{01}\left(\frac{1}{\Delta^2} + 2\Delta - 3\right) \quad (3)$$

$$S_1 = \frac{F}{A_0} = \frac{dW^{M-R}}{d\Delta} = 2(C_{10}\left(\Delta - \frac{1}{\Delta^2}\right) + (C_{01}\left(1 - \frac{1}{\Delta^3}\right) = 2\left(1 - \frac{1}{\Delta^3}\right)(\Delta C_{10} + C_{01}) \quad (4)$$

$$E_0 = 3G_0 = 6(C_{10} + C_{01}) \quad (5)$$

$$G_0 = 2(C_{10} + C_{01}) \quad (6)$$

$$\Delta = \frac{L}{L_0} = \varepsilon + 1 \quad (7)$$

Here, $W^{(M-R)}$ is the strain energy function of the hyper elastic material, S_1 is the stress, E_0 is the young modulus, G_0 is the shear modulus, ε is the strain, L is the length after loading and L_0 is the initial length. C_{10} and C_{01} are the coefficients of Mooney-Rivlin Theory. C_{01} was calculated as -0.05 and C_{10}, as 0.47, based on the experimental results of a previous study [11].

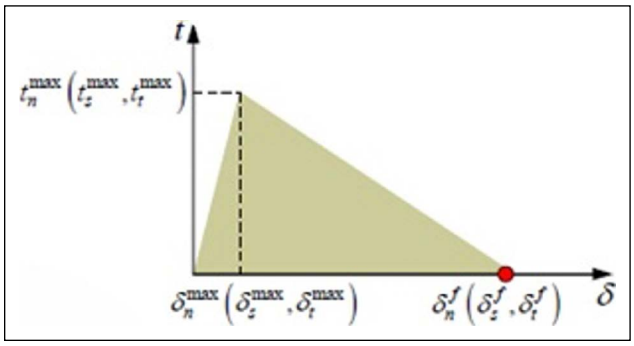

Figure 9. Traction separation laws [13].

For epoxy binder Sikadur 30 is used. The modulus of elasticity, Poisson's ratio, ultimate strain of Sikadur 30 is 1308MPa, 0.36, 3.8% respectively. The properties of this material can be seen in a previous study. Also, in that study it's said that epoxy can be assumed as a linear-elastic material [10]. So, in this study epoxy is considered as a linear elastic material which behaves linear until the stress of 49.7 MPa and after that it fails. This approach is consistent also with a previous study where epoxy's stress-strain curves are shown [12].

2.1.5. Modelling of The Interaction Between Binder and Materials

In Abaqus, one way for modelling the interaction between binders and materials is using surfaced based cohesive behaviour. Surface based cohesive behaviour allows an approach for modelling connections with negligibly small interface thickness, using the traction separation constitutive model. The surface based cohesive behaviour formulae are very similar to those used for cohesive elements with traction separation behaviour [13]. Traction separation laws are used to define the behaviour of joints in tension and shear failure modes (Fig. 9). When the assembly was first loaded, the joint performs a linear elastic behaviour, and K_n, K_s, K_t expresses the stiffness of the joint. After the peak traction value, the plastic response of joint starts. t_n^{max}, t_s^{max}, t_t^{max} are the maximum values of stress, δ_n^{max}, δ_s^{max}, δ_t^{max} are separation values at the maximum stress and, δ_n^f, δ_s^f, δ_t^f are the separations at failure as shown in Figure 9 [13].

Damage initiation was defined using the maximum nominal stress criterion. In mortar situation, the joint's tensile strength was assumed to be 0.173MPa. Cohesion coefficient was set to zero and pressure was multiplied by the coefficient of friction in the Mohr-Coulomb behaviour model (0.66). To characterize the behaviour following joint failure, the Mohr-coulomb shear sliding behaviour was defined with a coefficient of friction equal to 0.66. Thus, if the shear stress rises above the critical shear stress, the joint will slide. The experiments were used to determine the joint's fracture energies. Modified fracture energy was 0.10N/mm for failure mode of mod 1 (tension) and 0.183N/mm for

failure mode of mod 2 (shear). All values were taken from experimental work of past study [4]. The formulas utilized for cohesive elements with traction separation behaviour and those used for surface-based cohesive behaviour were extremely similar, as stated in the Abaqus manual [13]. The region under the traction-separation graph, known as the fracture energy, was therefore considered to be constant. The Benzeggagh-Kenane rule was used to capture the mixed mode behaviour in Abaqus. According to results from a previous study, when there is no difference between the critical fracture energies of second and third mode shear failures, the Benzeggagh-Kenane mode is the best choice for capturing the critical mixed mode fracture energy. According to the same study's recommendations for brittle behaviour, the Benzeggagh-Kenane exponent was chosen to be 2 [14].

The fracture energies of flexible joints and mortar joints were examined in a past study, which demonstrated that polymer joints have significantly higher damage and overall fracture energy [15]. Their analysis yielded polyurethane joint fracture energies of 4.22N/mm and 10.93 N/mm for first and second mode behaviour, respectively [4, 15]. For epoxy situation, based on the experimental results of joint failure of CFRP and brick in shear mode, as stated in a previous study K_s, K_t values are assumed 15 N/mm^3 and the fracture energy in shear mode was taken as 0.103N/mm [10]. Here, for the analysis in this study, tensile rigidity is assumed as half of the shear rigidity, so, K_n value is assumed as 7.5N/mm^3.

2.1.6. Finite Elements of The Frame

C3D8R elements were used for solid elements like concrete, homogenized infill wall, mortar, polyurethane and epoxy binders in the modelling. Rebars inside the RC frame was modelled using wires which are available in Abaqus for modelling solid elements whose cross-sectional dimensions are too small compared with its length. C3D8R elements are 8 node cube elements with reduced integration. The mesh of the model with panels is seen in Figure 10.

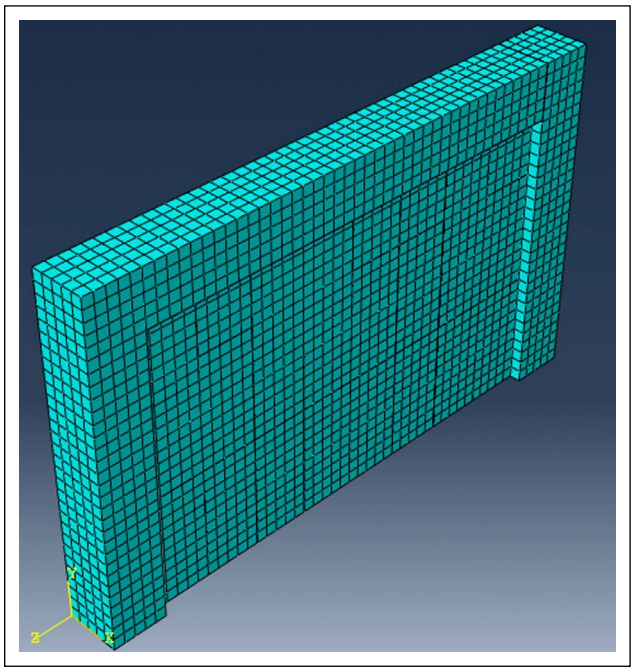

Figure 10. Mesh of model with panels.

3. RESULTS AND DISCUSSION

3.1. Load Displacement Curves

Bare frame carried maximum lateral load of 42757 N. The initial stiffness of the frame can be calculated by using the slope of the curve. For this purpose, the load of 32918 N is chosen because at this load linear part of the load-displacement curve finishes. The initial stiffness of the frame can be assumed as 11841N/mm. The traditionally infilled frame carried a total load of 50591N. This means a 18% increase if it is compared with bare frame. Normally a higher load can be expected, but the wall was considered to be constructed by putting the hollow bricks vertically to represent the weakest situation in practice. The initial stiffness of the frame can be considered as 19362N/mm if 33109N load is considered as the load where linear-elastic behaviour finishes. This means a 63% increase in initial lateral stiffness when compared with bare frame.

In the third frame in which infill walls were strengthened with 12.5mm panels, the maximum lateral load was 202559N. In this frame the panels near the RC frame were assumed to be anchored to the frame. As the binder material epoxy was used. The frame's lateral load carrying capacity was 4.73 times of bare frame and 4 times of traditionally infilled frame. The initial stiffness of frame was 61996.41 N/mm. This was 3.20 times of traditionally infilled frame. In the 4th frame to see the effect of anchorage, no panels were assumed to be anchored to RC frame. When compared with the third frame lateral load capacity slightly decreased to 188783.2 N. However, after maximum load the frame's ductility was not as high as the third frame. The anchorage provides higher energy consumption in large lateral displacements. Also, the initial stiffness of the frame decreased to 50000N/mm level.

In the fifth frame in which infill walls were strengthened with 12.5mm panels, the maximum lateral load was 147728.5N. In this frame the panels near the RC frame were assumed to be anchored to the frame. As the binder material polyurethane binder (polymer) was used. The polyurethane binder decreased the initial stiffness when compared with epoxy situation in the third frame, however the behaviour of the frame behaved in a ductile way in large deformations. The initial stiffness was 32767.22N/mm which is approximately the half of 3rd frame. Using polymer binder instead of epoxy decreased the maximum load carried by 37%. But still the lateral load capacity of the frame was nearly 3 times of the frame with traditional infill. In the sixth frame the effect of anchorage is investigated when polymer binder is used. For this purpose, no anchorage was used for any panels. The maximum lateral load carried by the frame was 116335.2N. This means 27% decrease in lateral load capacity when compared with fifth frame just because the panels were not anchored to RC frame. The initial stiffness of

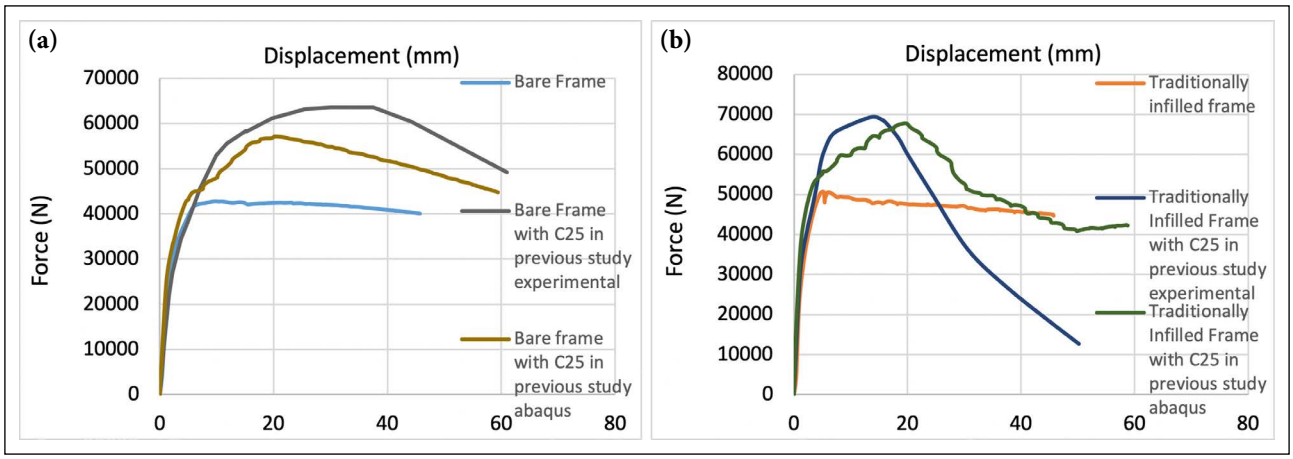

Figure 11. **(a)** Lateral load- lateral displacement curve of bare frame; **(b)** Lateral load-lateral displacement curve of traditional frame.

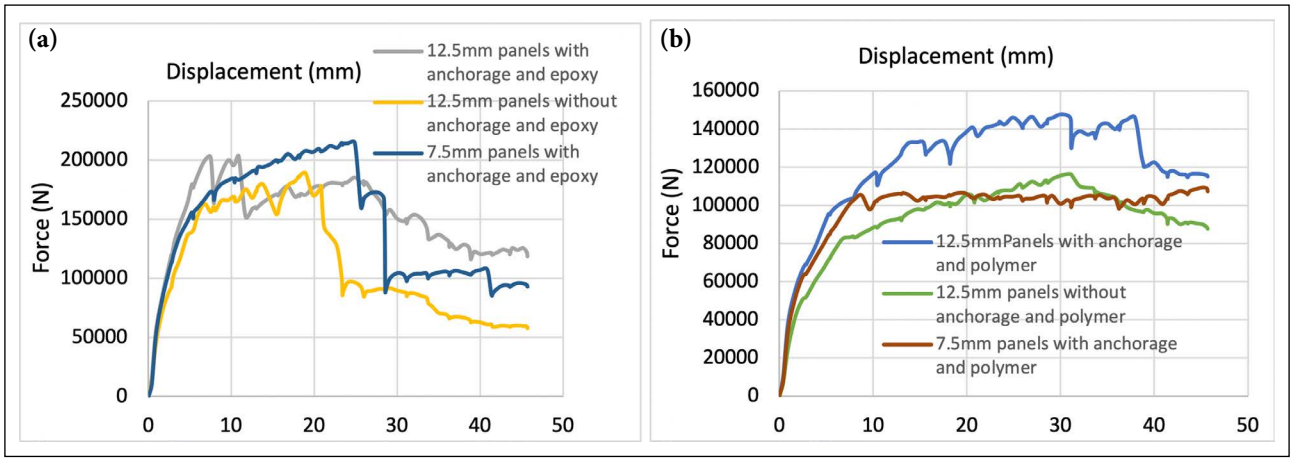

Figure 12. **(a)** Lateral load- lateral displacement curve of frames with epoxy; **(b)** Lateral load-lateral displacement curve of frames with polymer.

the frame decreased to 24473N/mm which indicates a 33% decrease with the anchorage situation. However, the lateral load capacity of the frame was 2.3 times of the frame with traditional infilled frame.

In the 7th and 8th frames, panels were changed with thinner ones to control the possibility of lowering the weight of the total frame. Because the panels were constructed with high strength fiber reinforced concrete with a compressive strength of 85.4 MPa. In these frames 7.5 mm thickness were assumed in the model for panels. In the seventh frame where epoxy binder was used the lateral load capacity was 214294.57N which is the highest of all models. The lateral load was increased by 5% when compared with thicker panels. However as seen in the graphs, by using thicker panels, after 30mm displacement more load can be carried. A sudden decrease in lateral load was observed around 30mm displacement in thinner panels situation. The initial stiffness of the frame can be assumed as same with 3rd frame. In the 8th frame thinner panels were compared when polymer binder was used. Lateral load capacity of the frame was decreased to 106080N from 147728.5N when panel thickness was decreased. But the lateral load capacity of frame was approximately 2 times more than the frame with traditional infill. The results can be seen in Figure 11, 12. According to the results, panel strengthening seems promising for seismic retrofit purposes.

3.2. Stress Analysis in The Frames

In Abaqus, after the analysis, equivalent Misses stresses can be seen. The Misses stresses in the components of the assembly (RC frame, infill wall, binder layer etc.) can be observed individually in the results section. In the bare frame analysis, in rebars, inside corner regions of the frame, equivalent misses stress reached to 550,9 MPa which indicates that rebars nearly failed. In the bay region of the beam the equivalent Misses stresses reached around 367MPa. In concrete material, Misses stresses reached 20–25 MPa in light blue regions on the corners. Then cracks and failure can be expected on those regions. Results are convenient if they are compared with the results of the bare frame with same dimensions from a previous study [4]. Results of the Misses stresses in concrete material can be seen in Figure 13. In traditionally infilled frame, in the infill wall, in the middle of the wall in a small zone the Misses stress reached 0.8Mpa. Around this zone, Misses stresses were around 0.55MPa to 0.41MPa. This indicates that they already exceeded the tensile strength of infill wall which is assumed as 0.25MPa.

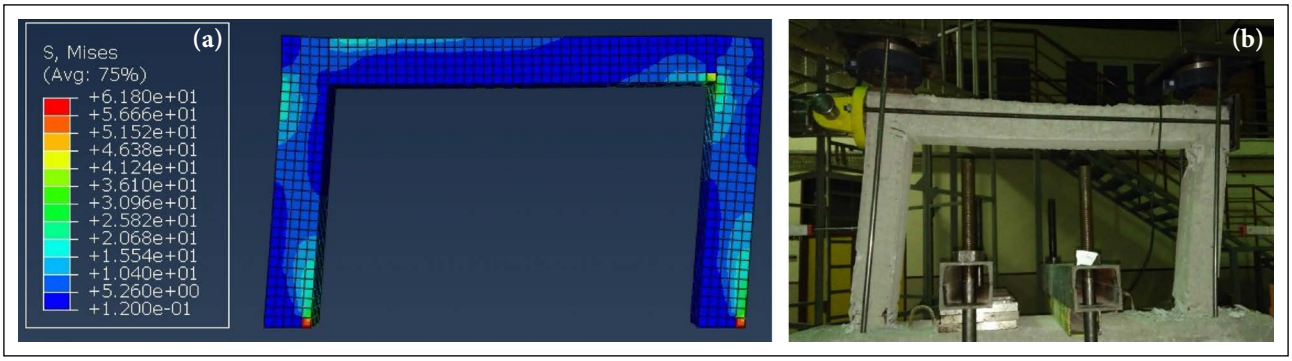

Figure 13. **(a)** Misses stress in bare frame's columns and beam; **(b)** Misses stress in bare frame in a previous experimental study[4].

In the third type of frame with anchored panels and epoxy binder, in the rebars, Misses stress distribution was slightly changed. In the corner regions of frame again the max. Misses stresses were observed as 522MPa. In the concrete of the frame, the stress distribution was changed when compared with traditionally infilled frame without panels. In some regions in the corners, it reached values like 89.2MPa, 59.5MPa, where the values are much beyond the strength of the material, which indicates that in these regions the material cracked. If the infill wall was observed separately, in the right corner at the bottom, in a big zone, equivalent Misses stresses reached 0.549MPa which is beyond the tensile strength of the material. So, demolition can be expected in that zone in infill wall. In the epoxy layer, maximum Misses stress was around 40 MPa which is smaller than the strength of the material, however it's loaded nearly up to limit. In the panels, the max Misses stress were around 5–10 MPa except some panels in the corners. The usage of high strength fiber reinforced lightweight concrete with 85.4 MPa compressive strength and 11.8MPa tensile strength prevented most of the panels to be cracked. In corner zones the stresses reached 40–50 MPa. Also, the separation of the panels from epoxy layer was observed and panels dropped.

In the fourth type of frame where panels were not anchored to RC frame, and epoxy binder was used, in the rebars, the maximum Misses stress was 542MPa in the tension zone of column ends, and around 361.8 MPa in the bay region of beam. The stress distribution was changed when compared with traditionally infilled frame without panels. In RC frame's concrete, cracking can be expected in the regions on the corners of frame 41.26 MPa Misses stress is higher than the concrete's strength. In infill wall of the frame, in bottom left corner of the loading side, and near the bottom region in the middle, Misses stresses reached 0.37–0.48MPa which exceeds the tensile strength of material. Cracks and failure were expected in the regions according to Misses stress. In the epoxy layers in backside and front side of walls, Misses stresses reached around 25 MPa which is lower than the epoxy strength. The Misses stresses in panels reached to a value of 29 MPa in the corner of frame. Panels at the top left corner especially, were separated from layer and dropped. All of the results can be seen in Figure 14–16.

In the situation of anchored panels and polymer binders (5^{th} type of frame), in rebars, maximum Misses stress was 532 MPa in tension zones of columns and beams. and around 355–400MPa values were seen in rebars at the bottom of beam. In the concrete of RC frame, cracking can be expected in the regions on the corner regions of frame where Misses stresses reached 25MPa in a wide region and reached 50.34MPa around the regions of loading. In the right corner in a small region, stresses reached even 75.48MPa. In the infill on the bottom left side especially the Misses stresses reached 0.49MPa which is higher than the tensile strength of material. In polymer material the maximum Misses stress was 1.74 MPa only in a small region, tearing off the material could be expected however deformation capacity of polymer is very high. Generally, beyond this region, in polymer material stresses does not exceed the tensile strength of the material. In especially in anchored panels at the bottom corner, high Misses stresses around 60 MPa was observed. These stresses are beyond the tensile strength of material. Therefore, cracking can be expected in these regions.

In the frame with panels without anchorage and polymer binder (6^{th} type of frame), in rebars, maximum Misses stress was 550 MPa in tension zones of columns. and around 367–412MPa values were seen in longitudinal rebars of beam and stir-ups of columns. In the concrete of RC Frame, on corner zones of frame, Misses stresses varied between around 20–40MPa. Damage happened on these corners. In the infill wall, Misses stresses reached 0.37 MPa at the top and bottom edges of wall. This stress exceeded the tensile strength of material so damage is expected on these zones. Polymer binder, when compared with epoxy counterpart, decreased the stresses in most regions of the infill especially in the frame without any panel anchored to RC frame. In the polymer layer in the infill wall, the maximum Misses stress is 1.14MPa which is smaller than the tensile strength of material (1.4MPa). In panels except regions around corners and bottom of frame, Misses stresses were around to be around 8 MPa which is smaller than the tensile strength of the material. On the corners stresses reached around 54.63 MPa. No separation between polymer layer and panels was observed. The results and Misses stress distribution can be seen in Figure 17–19.

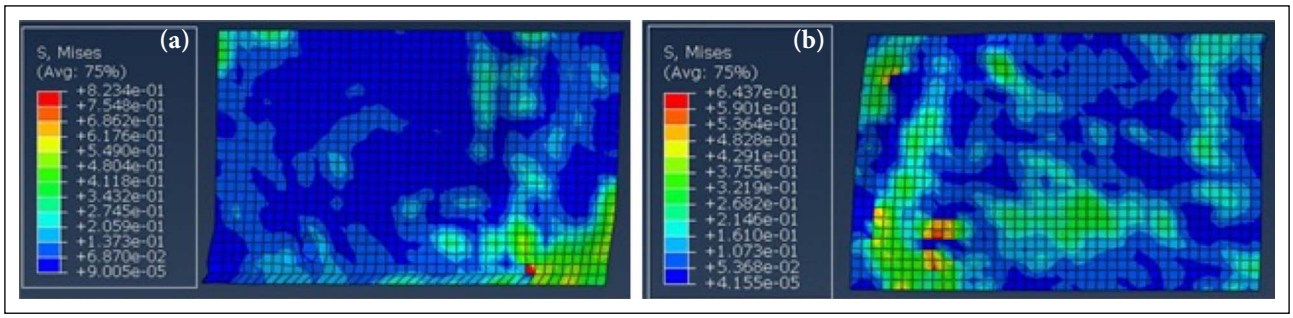

Figure 14. **(a)** Misses stress in 3rd frame's infill wall; **(b)** Misses stress in 4th frame's infill wall.

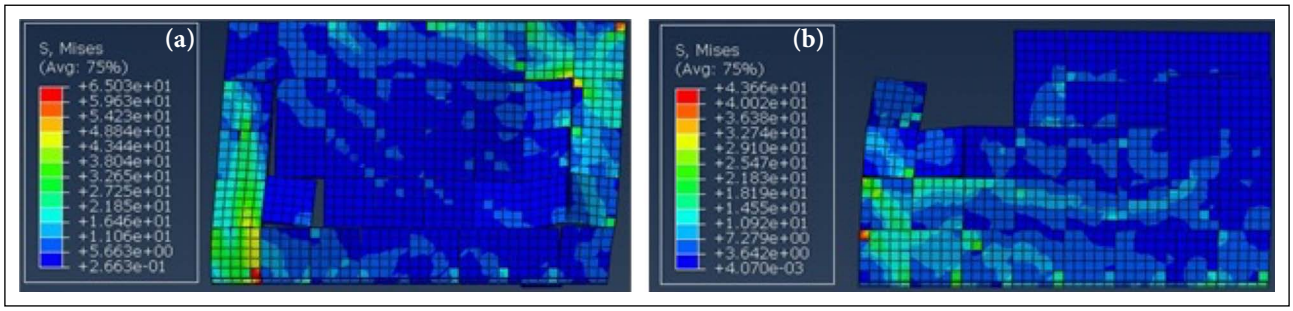

Figure 15. **(a)** Misses stress in 3rd frame's panels; **(b)** Misses stress in 4th frame's panels.

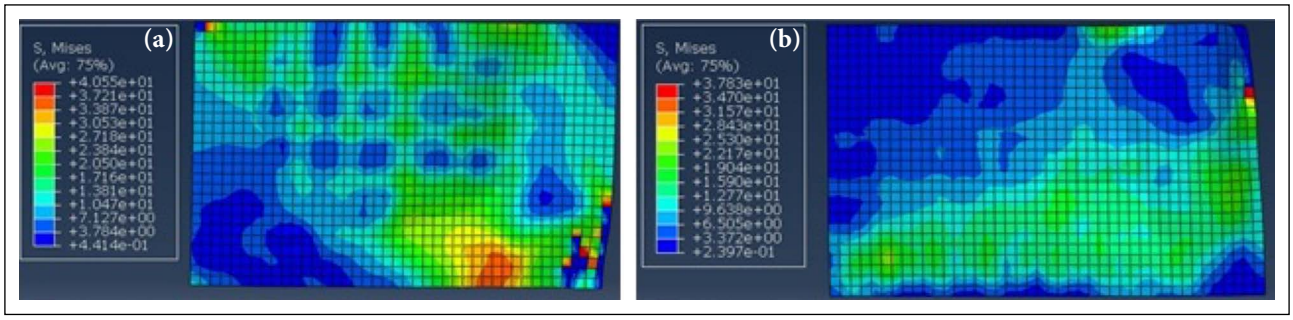

Figure 16. **(a)** Misses stress in 3rd frame's epoxy layer; **(b)** Misses stress in 4th frame's epoxy layer.

In the 7th type of frame with 7.5mm panels and epoxy, in rebars maximum Misses stress was 526MPa in column longitudinal rebars and stir-ups. In the concrete of RC frame, Misses stress distribution was similar with previous frames. In the infill wall of this frame, at the corner zones of frame, Misses stresses varied between 0.37–0.64 MPa which is higher than the tensile strength of material. But in most parts of infill wall stresses were lower than the tensile strength of 0.25MPa. Damage can be expected in corner zones. In the epoxy layer, the Misses stresses were around 31MPa in wide regions around the top and bottom corner zones. This is lower than the strength of material. Again, the separation of panels from epoxy was observed and many panels were dropped from wall. The Misses stresses were around to be around 52–59 MPa around corner regions of frame.

In the 8th type of frame with 7.5mm panels and epoxy, in rebars maximum Misses stresses reached 541MPa in column and around 360MPa in beam. In the concrete of RC frame, Misses stress distribution was similar with previous frames. In the polymer layer of the frame maximum Misses stress was slightly higher than the tensile strength of material (1.4MPa) with a value of 1.44MP only in a small zone existing vertically. In the infill wall of this frame, at the top and bottom parts of the wall, Misses stresses were around 0.4–0.5 MPa which is higher than the tensile strength of material. But in most parts of infill wall stresses were lower than the tensile strength of 0.25MPa. In panels except regions around corners and bottom of frame, Misses stresses were around to be around 6.70MPa which is smaller than the tensile strength of the material. On the corners stresses reached around 52.86 MPa mostly and no separation between polymer layer and panels was observed. All of the results can be seen in Figure 20–22.

3.3. Evaluation of Results

The method proposed here can be compared with the retrofitting method by using CFRP proposed by past studies [1, 16]. In one of these studies, experimental work was performed, and in the other one, a numerical analysis was performed with the results of experiments by proposing a behavior model for the idealization of load-displacement curves.

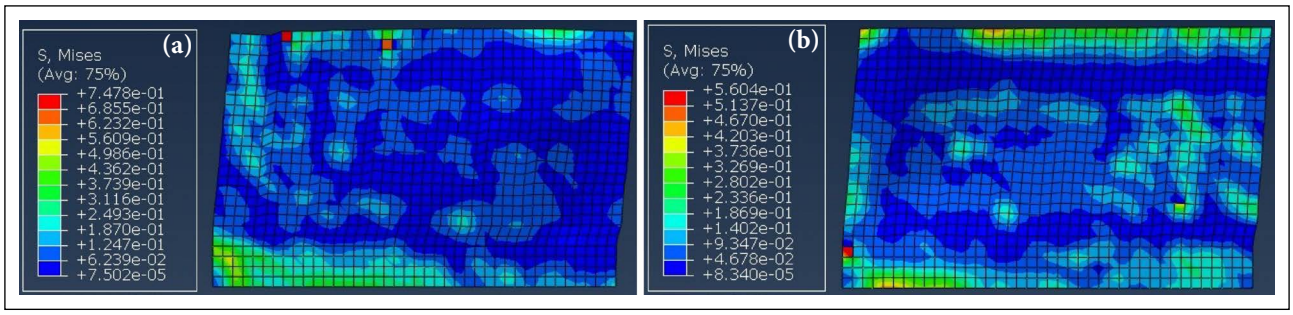

Figure 17. **(a)** Misses stress in 5th frame's infill wall; **(b)** Misses stress in 6th frame's infill wall.

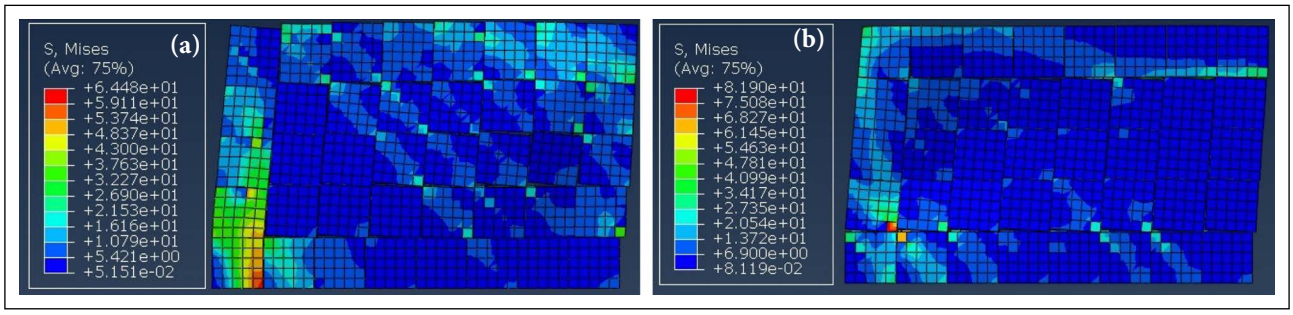

Figure 18. **(a)** Misses stress in 5th frame's panels; **(b)** Misses stress in 6th frame's panels.

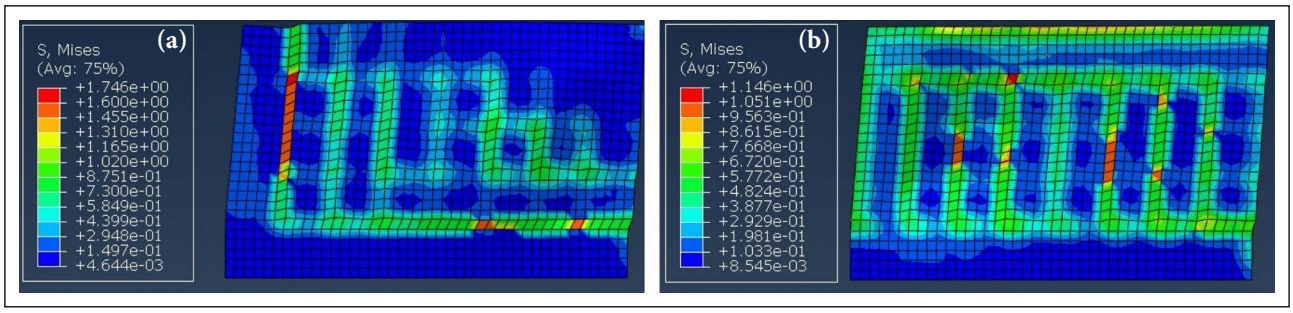

Figure 19. **(a)** Misses stress in 5th frame's polymer layer; **(b)** Misses stress in 6th frame's polymer layer.

Before comparing the behavior of retrofitted specimens, it would be reasonable to compare the results of non-retrofitted traditionally infilled RC frames with the experimental results of past studies [16]. In the past study, 1/3 scaled RC frames were constructed with a bay length of 933mm and a column height of 1 m. The column and beam dimensions were 100 x200mm, and concrete with a compressive strength of 19MPa (cylinder) was used. The steel material used for reinforcement bars had a yielding stress of 420MPa and ultimate stress of 500MPa. The features of the specimens were quite similar to the frame used here. Six different RC frame specimens were constructed. One was an ordinary specimen with traditional hollow brick infills, and the others were retrofitted using CFRP. The RC frames were subjected to cyclic loading until approximately a 4–6% drift ratio. According to the lateral load-displacement curves, RC Frame with a traditional infill wall without retrofit carried a 120 KN maximum load. If Figure 11 is observed, it can be seen that the traditionally infilled frame showed similar behavior to the frame of the past study [4]. It is worth mentioning that the result of the numerical analysis done in the previous study [4] for traditionally infilled frames is also consistent with the load-displacement graph in the other experimental study [16]. However, the concrete used in this study is a low-strength concrete different than the mentioned studies, which is why it carried 50591N maximum load, which is smaller than past studies. These results show that Abaqus's analysis of traditionally infilled frames is consistent with two past studies [4, 16].

Diamond cross-braced retrofitting with CFRP increased the lateral load capacity of RC frame by 1,69 times compared with the traditionally infilled frame in the past study [16]. However, in this study, the proposed method increased the lateral load-carrying capacity of the RC frame by 4.29 times.

Maximum story drift corresponding to maximum load was around 0.5%–1,10% in CFRP retrofitted frames in the past study [16]. This result is reasonable compared to the other study where some data is compiled from literature, and the following statement was written: "For bare infills, the average drift corresponding to the ultimate strength was in the range of 0.90–1.00 %. The aver-

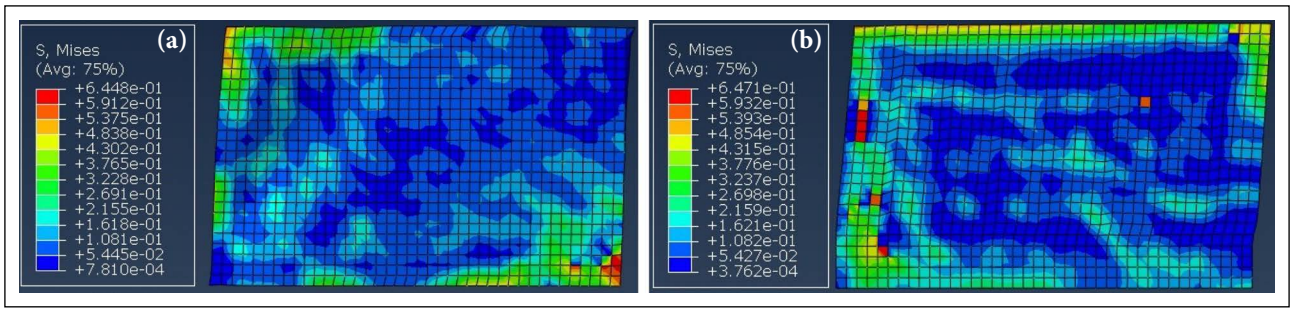

Figure 20. **(a)** Misses stress in 7th frame's infill wall; **(b)** Misses stress in 8th frame's infill wall.

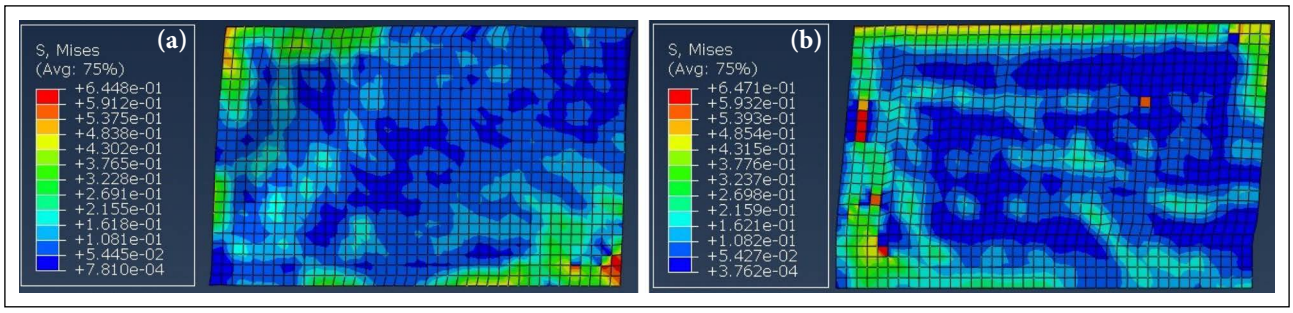

Figure 21. **(a)** Misses stress in 7th frame's panels; **(b)** Misses stress in 8th frame's panels.

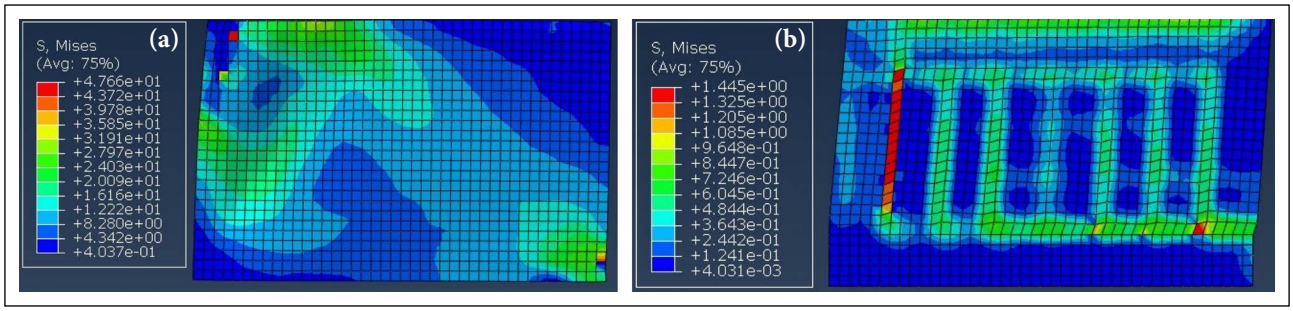

Figure 22. **(a)** Misses stress in the 7th frame's epoxy layer; **(b)** Misses stress in the 8th frame's polymer layer.

age drift corresponding to the ultimate strength for the retrofitted infills was 0.70–1.15 %. (CFRP retrofitted)" [1]. In this study, the best specimen with 7.5mm panels drift corresponding to maximum load is 0.0293%. So, the proposed retrofitting method here allowed more lateral drift corresponding to maximum load. However, a more critical aspect is that, especially in the case of a polymer, the behavior of frames in this study is very ductile until the lateral drift of 6%. The specimens continued to carry loads even in large drifts. In the past study with CFRP retrofitting, the experimental results showed that ultimate strains for retrofitted frames were around 2,5–4%.

As mentioned before, the initial stiffness of the traditionally infilled frame can be considered as 19362N/mm in this study. In the best case, the proposed retrofitting here with panels and epoxy increased the initial stiffness of the RC frame to 61996.41 N/mm. This indicates an increase of 3.20 times compared to the traditionally infilled frame. The CFRP retrofitting in the past study increased the initial stiffness of the RC frame by 3.11–4.03 times in the best cases to a range of 39800–55600N/mm [16]. The results show that the proposed retrofitting method with panels increases the initial stiffness of frames as much as CFRP retrofitting.

In the other study, for CFRP retrofitted specimens, a piecewise linear capacity curve model was proposed by using the hysteresis curves of past studies [1]. The model was validated by comparing the numerical results with experimental results of 1/3 scaled one-story frames. Also, another independent comparison was performed for two story frames. After verification of results, the model was used to analyze an existing structure. It was seen that the CFRP retrofitting increased the total base shear of the structure from 1750KN to 9600KN in the X direction and from 2300 KN to 7700KN in the Y direction. This indicates an increase of 5.48–3.34 times in the X and Y directions.

In this study, a formerly proposed idea was improved. In the formerly proposed method, precast panels were used to strengthen the frames with the help of an epoxy binder. In the previous study, where an experimental study was conducted with 1/3 scaled frames, precast panels were used for strengthening, and lateral load capacity increased from 65.5–86.6 KN to 148.9–254.7KN levels. This indicates an increase of 3.88 times in the best case [2]. According to the results of that study, when the epoxy

binder was used, in the best case, the RC frame's lateral load-carrying capacity increased by 4.29 times when compared with the traditionally infilled RC frame. A polymer binder can be used to achieve ductile behavior in large lateral drifts after a 3% lateral drift ratio. In the best case with a polymer binder, the RC frame's lateral load-carrying capacity increased by three times when compared with the traditionally infilled RC frame.

4. CONCLUSION

In this study, an attempt was made for a practical seismic retrofit method. Infill walls were strengthened using high-strength lightweight concrete panels for that purpose. High-strength, lightweight concrete panels can be constructed quickly, and the production process does not need sophisticated methods. Also, different kinds of binders were used to apply panels to the infill walls. The results of load-displacement curves show that the proposed method is a prospect for the future. It allows retrofitting structures using 0.5m x 0.5m concrete panels with a 3cm thickness only, and careful crafting or leaving the house during the retrofit process is unnecessary. When epoxy binder was used, in the best case, the RC frame's lateral load-carrying capacity increased by 4.29 times compared to the traditionally infilled RC frame. Polymer binder can be used to achieve ductile behavior in large lateral drifts after 3% lateral drift ratio. In the best case with a polymer binder, the RC frame's lateral load-carrying capacity increased by three times when compared with the traditionally infilled RC frame. In the best case, the proposed retrofitting here with panels and epoxy increased the initial stiffness by 3.20 times compared to the traditionally infilled frame.

The stress analysis shows that most high-strength lightweight concrete panels could bear the stresses during loading, even in large drifts. However, for some regions, optimization can be performed in the future. With proper optimization, the behavior can be improved. The stresses in a polymer binder are lower than the strength of the material. The panels are not separated from the wall, even with a sizeable lateral drift of 6%. This is important to protect people from falling walls during strong earthquakes.

ETHICS

There are no ethical issues with the publication of this manuscript.

DATA AVAILABILITY STATEMENT

The authors confirm that the data that supports the findings of this study are available within the article. Raw data that support the finding of this study are available from the corresponding author, upon reasonable request.

CONFLICT OF INTEREST

The authors declare that they have no conflict of interest.

FINANCIAL DISCLOSURE

The authors declared that this study has received no financial support.

PEER-REVIEW

Externally peer-reviewed.

REFERENCES

[1] Özkaynak, H., Sürmeli, M., & Yüksel, E. (2016). A capacity curve model for confined clay brick infills. *Bull Earthquake Engineering* 14(3), 889–918. [CrossRef]

[2] Baran, M., Canbay, E., & Tankut, T. (2010). Beton panellerle güçlendirme - kuramsal yaklaşım. *Teknik Dergi*, 21(101), 4959-4978.

[3] Kwiecien, A. (2013). Highly deformable polymers for repair and strengthening of cracked masonry structures. *International Journal of Engineering Technology*, 2(1), 182-196. [CrossRef]

[4] Koman, H. (2021). *Harçsız bloklar kullanılarak yapıların deprem davranışının iyileştirilmesi*. [Doctoral dissertation].

[5] Demir, C. (2012). *Seismic behaviour of historical stone masonry*. (Publication No. 501032106) [Doctoral dissertation, Istanbul Technical University].

[6] Santos, C. F. R., Alvarenga, R. C. S. S., Riberio, J. C. L., Castro, L. O., Silva, R. M., Santos, A. A. R., & Nalon, G. H. (2017). Numerical and experimental evaluation of masonry prisms by finite element method. *Ibracon Structure and Materials Journal*, 10(2), 477-508. [CrossRef]

[7] Obaidat, Y. T. (2011) *Structural retrofitting of concrete beams using FRP*. [Doctoral dissertation, Lund University].

[8] Mosallam, AS, Ghabban, N, Mirnateghi, E, & Agwa, AAK. (2022). Nonlinear numerical simulation and experimental verification of bondline strength of CFRP strips embedded in concrete for NSM strengthening applications. *Structural Concrete*, 23, 1794–1815. [CrossRef]

[9] Gao, J., Sun, W., & Morino, K. (1997). Mechanical properties of steel fiber-reinforced, high-strength, lightweight concrete. *Cement and Concrete Composites*, 19(4), 307-313. [CrossRef]

[10] Kwiecien, A. (2014). Shear bond of composites to brick applied highly deformable in relation to resin epoxy interface materials. *Materials and Structures*, 47, 2005-2020. [CrossRef]

[11] Ksiel, P. (2018). *Model approach for polymer flexible joints in precast elements joints for concrete pavements*. [Doctoral dissertation, Cracow University of Technology].

[12] Nekliudova, E.A., Semenov, A.S., Melnikov, B.E., & Semenov, S.G. (2014). Experimental research and finite element analysis of elastic and strength properties of fiberglass composite material. *Magazine of Civil Engineering*, 47(3), 25–39. [CrossRef]

[13] Dassault Systems. Simula ABAQUS, Modelling fracture and Failure, Lecture 6. https://www.3ds.com/products-services/simulia/training/course-descriptions/modeling-fracture-and-failure-with-abaqus/.

[14] Abdulla, K. F., Cunningham, L. S., & Gillie, M.

(2017). Simulating masonry behaviour using a simplified micro model approach. *Engineering Structures*, 151, 349-365. [CrossRef]

[15] Viskovic, A., Zuccarino, L., Kwiecien, A., Zajac, B., Gams, M. (2017). Quick seismic protection of weak masonry infilling in filled frame structures using flexible joints. *Key Engineering Materials*, 747, 628-637. [CrossRef]

[16] Yuksel, E., Ozkaynak, H., Buyukozturk, O., Yalcin, C., Dindar, A.A., Surmeli, M., & Tastan, D. (2010). Performance of alternative CFRP retrofitting schemes used in infilled RC frames. *Construction and Building Materials,* 24(4), 596-609. [CrossRef]